

Chain-growth simulations of lattice-peptide adsorption to attractive substrates

Michael Bachmann and Wolfhard Janke

Institut für Theoretische Physik,
Universität Leipzig, 04109 Leipzig, Germany
E-mail: {bachmann, janke}@itp.uni-leipzig.de

Based on a newly developed contact-density chain-growth algorithm, we have simulated a non-grafted peptide in the vicinity of different attractive substrates. We analyzed the specificity of the peptide adsorption by focussing on the conformational transitions the peptide experiences in the binding/unbinding processes. In a single simulation run, we obtained the contact density, i.e., the distribution of intrinsic monomer-monomer contacts and monomer-substrate nearest-neighbor contacts. This allows a systematic reweighting to all values of external control parameters such as temperature and solvent quality after the simulation. The main result is the complete solubility-temperature pseudo-phase diagram which is based on the corresponding specific-heat profile. We find a surprisingly rich structure of pseudo-phases that can roughly be classified into compact and expanded conformations in both regimes, adsorption and desorption. Furthermore, underlying subphases were identified, which, in particular, appear noticeably in the compact pseudo-phases.

1 Introduction

In recent experiments it could be shown that the affinity of peptides to self-assemble at metal¹ and semiconductor substrates²⁻⁴ is highly influenced by the amino acid content of the peptide, the order of the residues within the sequence, the specific substrate, and its crystal orientation at the surface.

In this study, we investigate the binding specificity with a minimalistic lattice model for the hybrid system of a peptide in the vicinity of an attractive substrate. Due to the specific properties of the peptide, this problem is distinguishingly different from the hybrid system of a (homo)polymer near an adsorbing substrate, which has already been extensively studied⁵⁻¹⁰. The peptide sequence consists of hydrophobic and polar residues, i.e., the 20 protein-building amino acids are classified into only two groups. The idea behind this hydrophobic-polar (HP) model¹¹ is that proteins usually possess a compact hydrophobic core surrounded by a shell of polar residues which screen the core from the aqueous environment. For this reason and for simplicity, only an effective, short-range attractive force between the hydrophobic monomers is employed. Furthermore, the peptide is restricted to live on a simple-cubic lattice. The volume exclusion of the side chains is simply taken into account by considering only self-avoiding linear chains. The energy of such a lattice peptide is related to the number of hydrophobic nearest-neighbor contacts, n_{HH} .

The power of this highly abstract model lies in its simplicity. Peptides with more than 100 residues can be studied – this is in striking contrast to refined all-atom protein models, where a systematic analysis of thermodynamic properties is only reliably possible for peptides with hardly more than 20 amino acids. It is expected that for longer peptides atomic details become less relevant and, therefore, simplified (“coarse-grained”) heteropolymer

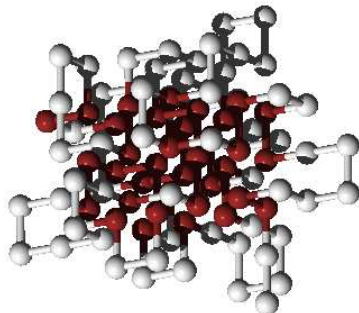


Figure 1. Putative ground-state conformation of the model peptide in the bulk (or in the desorbed pseudo-phase).

models can give satisfying qualitative answers to specific questions, e.g., regarding tertiary conformational transitions^{15,16}, and systematic sequence analyses¹⁷.

2 Lattice peptide and hybrid system model

As a model peptide, we use the HP transcription of the 103-residue protein *cytochrome c*, which was extensively studied in the past^{12–14,18}. We have first performed a detailed analysis of this model peptide in the bulk¹⁸ by applying the newly developed multicanonical chain-growth algorithm¹⁵. This method allowed the precise determination of the density of states for this system covering more than 50 orders of magnitude. The lowest-energy conformation we identified¹⁸ possesses 56 hydrophobic contacts (see Fig. 1) and exhibits a degeneracy of the order of 10^{16} . It is therefore likely that there still exist lower-lying energetic states.

Here, this lattice peptide resides in a cavity with an attractive substrate. In order to study the specificity of residue binding, we distinguish three substrates with different affinities to attract the peptide monomers: (a) the type-independent attractive, (b) the hydrophobic, and (c) the polar substrate. The number of corresponding nearest-neighbor contacts between monomers and substrate shall be denoted as n_s^{H+P} , n_s^H , and n_s^P , respectively. The energy (in arbitrary units) of the hybrid system is then given by

$$E_s(n_s, n_{\text{HH}}) = -n_s - sn_{\text{HH}}, \quad (1)$$

where $n_s = n_s^{H+P}$, n_s^P , or n_s^H , depending on the substrate. Besides the temperature T , the solubility (or reciprocal solvent parameter) s is an external control parameter which governs the quality of the solvent (the larger the value of s , the worse the solvent). The simulation of this model is based on a recently developed contact-density chain-growth algorithm¹⁰ which allows a direct estimation of the degeneracy (or contact density) $g(n_s, n_{\text{HH}})$ of macro-states of the system with given contact numbers n_s and n_{HH} .

3 Contact-density chain-growth algorithm

The contact-density chain-growth algorithm is a suitably enhanced version of the multicanonical chain-growth algorithm¹⁵, which is based on the pruned-enriched variant¹⁹ of

the Rosenbluth chain-growth method²⁰. In contrast to move-set based Metropolis Monte Carlo or conventional chain-growth methods which would require many separate simulations to obtain results for different parameter pairs (T, s) and which frequently suffer from slowing down in the low-temperature sector, our method allows the computation of the *complete* contact density for each system within a *single* simulation run. Since the contact density is independent of temperature and solubility, energetic quantities such as the specific heat can easily be calculated for all values of T and s (nonenergetic quantities require accumulated densities to be measured within the simulation, but this is also no problem). For all systems, 10 independent runs were initialized, each generating 10^8 conformations.

In order to regularize the influence of the unbound conformations and for computational efficiency, the heteropolymer is restricted to reside in a cage, i.e., in addition to the physically interesting attractive surface there is a steric, neutral wall parallel to it in a distance z_w . The value of z_w is chosen sufficiently large to keep the influence on the unbound heteropolymer small (in this work we used $z_w = 200$).

4 Pseudo-phase diagram of conformational transitions

Our main interest is devoted to the conformational transitions the peptide experiences in the binding or adsorption process to the substrates. For a first overview, it is convenient to study the specific heat C_V as a function of the external parameters temperature T and solubility s . Respective ridges and peaks of the specific heat can be considered as signals of conformational activity. Due to the fixed length of the peptide sequence, a conventional discussion of thermodynamic phase transitions (e.g., in terms of finite-size scaling) is not possible. It should also be noted that the behavior of *finite* polymer and peptide systems in future nanotechnological applications will be of essential interest as a consequence of the need for maximally possible space reduction, e.g., for nanoelectronic circuits. In such cases, subphase crossover transitions, which are of marginal or no importance in large systems, strongly influence the self-assembling structure of the polymer or peptide at the substrate.

In Figs. 2(a)-(c) the color-coded profiles of the specific heats for the different substrates are shown (the brighter the colour, the larger the value of C_V). We interpret the ridges (for accentuation marked by white and gray lines) as the boundaries of the pseudo-phases. It should be noted, however, that in such a finite system the exact positions of active regions exhibited by fluctuations of other quantities usually deviate, but the qualitative behavior is similar.¹⁵ Despite the surprisingly rich and complex phase behavior there are main “phases” that can be distinguished in all three systems. These are separated in Figs. 2(a)-(c) by gray lines. Comparing the three systems we find that they all possess pseudo-phases, where adsorbed compact (AC), adsorbed expanded (AE), desorbed compact (DC), and desorbed expanded (DE) conformations dominate, similar to the generic phase diagram of a homopolymer¹⁰. “Compact” here means that the heteropolymer has formed a dense hydrophobic core, while expanded conformations form dissolved, random-coil-like structures. The sequence and substrate specificity of heteropolymers generates, of course, new interesting and selective phenomena not available for homopolymers. One example is the pseudo-phase of adsorbed globules (AG), which is noticeably present only in those systems, where all monomers are equally attractive to the substrate (Fig. 2(a)) and where polar monomers favour contact with the surface (Fig. 2(b)). In this phase, the con-

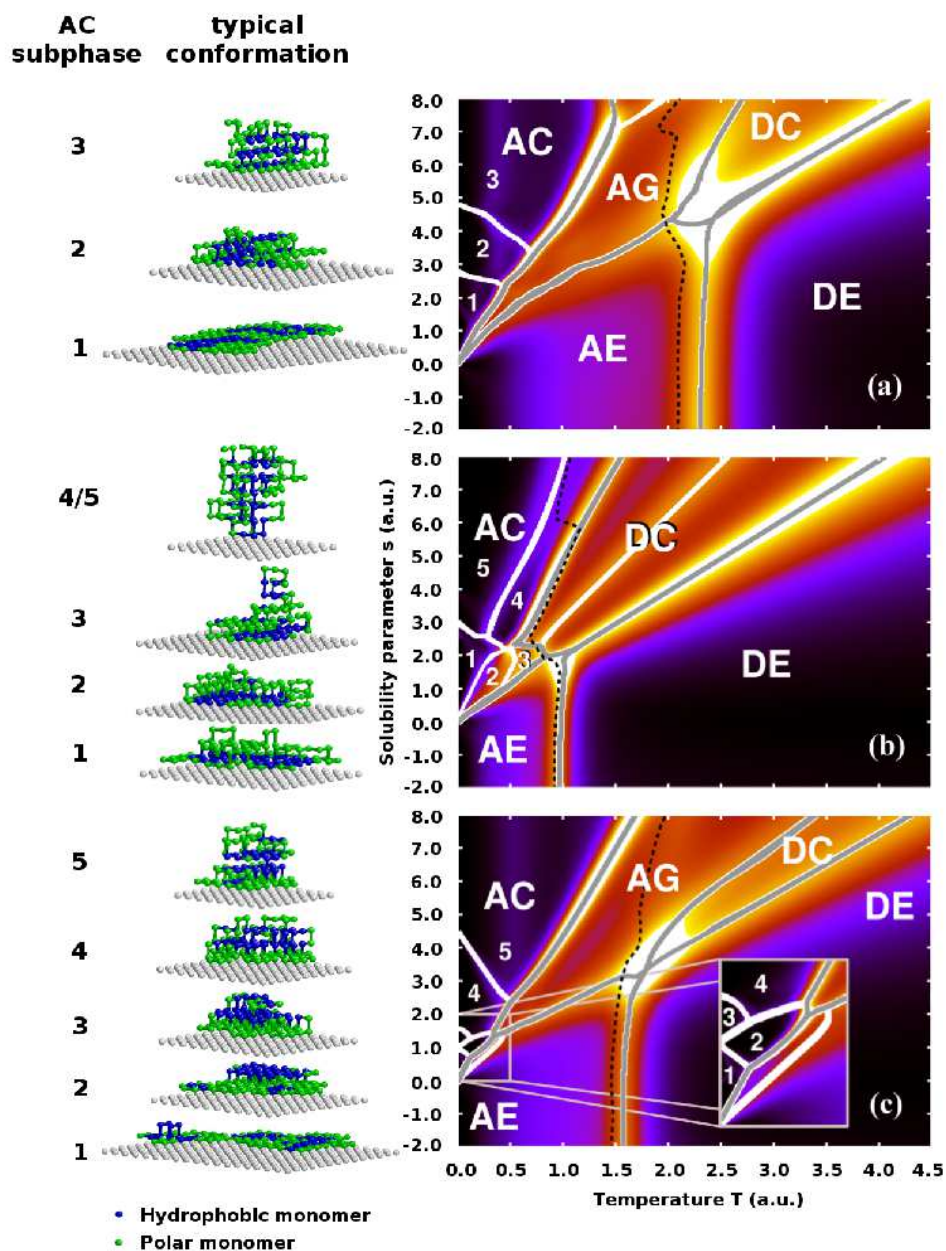


Figure 2. Specific-heat profiles as a function of temperature T and solubility parameter s of the 103-mer near three different substrates that are attractive for (a) all, (b) only hydrophobic, and (c) only polar monomers. White lines indicate the ridges of the profile. Gray lines mark the main “phase boundaries”. The dashed black line represents the first-order-like binding/unbinding transition state, where the contact free energy possesses two minima (the adsorbed and the desorbed state). In the left panel typical conformations dominating the associated AC phases of the different systems are shown.

formations are intermediates in the binding/unbinding region. This means that monomers currently desorbed from the substrate have not yet found their position within a compact conformation.

The strongest difference between the three systems is their behavior in pseudo-phase AC, which is roughly parameterized by $s > 5T$. Representative conformations for all AC subphases are shown in the left panel of Fig. 2. If hydrophobic and polar monomers are equally attracted by the substrate (Fig. 2(a)), we find three AC subphases in the parameter space plotted. In AC1 film-like conformations dominate, i.e., all 103 monomers are in contact with the substrate. The formation of a single, compact hydrophobic core proceeds by layering transitions from AC1 to AC3 via AC2. The reason for the existence of phase AC2 is the reduced cooperativity of the polar monomers due to their surface attraction. In AC3, the heteropolymer has maximized the number of hydrophobic contacts and only local arrangements of monomers on the surface of the very compact structure lead to the still possible maximum number of substrate contacts.

The AC heteropolymer conformations adsorbed at a surface that is only attractive to hydrophobic monomers (Fig. 2(b)) depend on two concurring hydrophobic forces: substrate attraction and formation of intrinsic contacts. The *single* film-like hydrophobic domain in AC1 is maximally compact, at the expense of displacing polar monomers into upper layers. In subphase AC2 intrinsic hydrophobic contacts are entropically broken, while AC3 exhibits hydrophobic layers at the expense of hydrophobic substrate contacts. A dramatic, highly cooperative, hydrophobic collapse accompanies the transitions from AC1 to AC4/5, where in a one-step process the compact two-dimensional domain transforms to the compact three-dimensional hydrophobic core.

Not less exciting is the subphase structure of the heteropolymer interacting with a polar substrate (Fig. 2(c)). For small values of s and T , the behavior of the heteropolymer is dominated by the concurrence between polar monomers contacting the substrate and hydrophobic monomers favouring the formation of a hydrophobic core, which, however, also requires cooperativity of the polar monomers. In AC1, film-like conformations with disconnected hydrophobic clusters dominate. Entering AC2, a second hydrophobic layer forms at the expense of a reduction of polar substrate contacts. In contrast to the case of a hydrophobic substrate (Fig. 2(b)), the strong surface attraction of polar monomers hinders here the formation of a compact hydrophobic core (AC2/3 to AC5) which results in the intermediate subphase AC4.

5 Free-energy landscape from a different perspective

The contact numbers n_s and n_{HH} are kind of order parameters adequately describing the macro-state of the system. With its degeneracy $g(n_s, n_{\text{HH}})$, we define the contact free energy as $F_{T,s}(n_s, n_{\text{HH}}) \sim -T \ln g(n_s, n_{\text{HH}}) \exp(-E_s/T)$ and the probability for a macro-state with n_s substrate and n_{HH} hydrophobic contacts as $p_{T,s}(n_s, n_{\text{HH}}) \sim g(n_s, n_{\text{HH}}) \exp(-E_s/T)$. Assuming that the minimum of the free-energy landscape $F_{T,s}(n_s^{(0)}, n_{\text{HH}}^{(0)}) \rightarrow \min$ for given external parameters s and T is related to the class of macro-states with $n_s^{(0)}$ surface and $n_{\text{HH}}^{(0)}$ hydrophobic contacts, this class dominates the phase the system resides in. For this reason, it is instructive to calculate all minima of the contact free energy and to determine the associated contact numbers in a wide range of values for the external parameters. The map of all possible free-energy minima in the range of

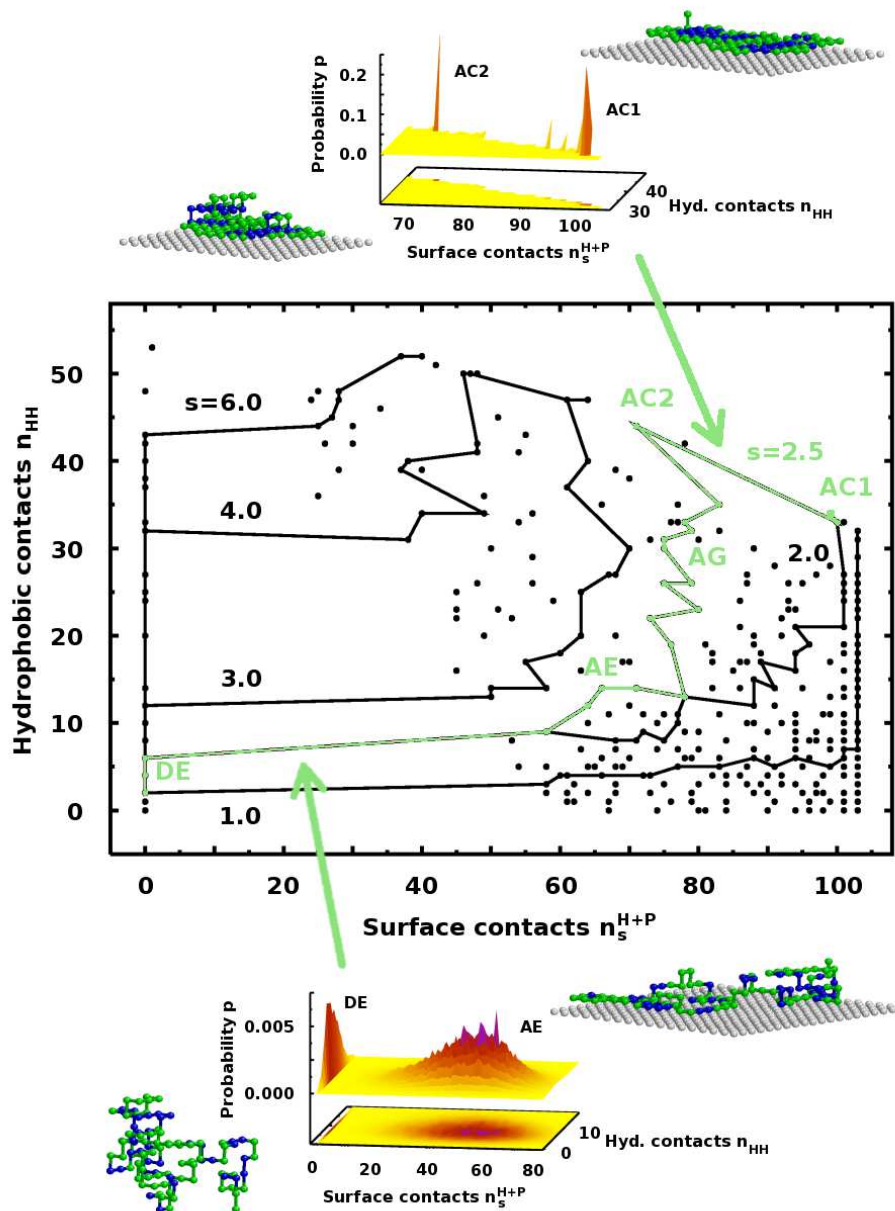


Figure 3. Contact-number map of all free-energy minima for the 103-mer and substrate equally attractive to all monomers. Full circles correspond to minima of the contact free energy $F_{T,s}(n_s^{H+P}, n_{HH})$ in the parameter space $T \in [0, 10]$, $s \in [-2, 10]$. Lines illustrate how the contact free energy changes with the temperature at constant solvent parameter s . For the exemplified solvent with $s = 2.5$, the peptide experiences near $T = 0.35$ a sharp first-order-like layering transition between single- to double-layer conformations (AC1,2). Passing the regimes of adsorbed globules (AG) and expanded conformations (AE), the discontinuous binding/unbinding transition from AE to DE happens near $T = 2.14$. In the DE phase the ensemble is dominated by desorbed, expanded conformations. Representative conformations of the phases are shown next to the respective peaks of the probability distributions.

external parameters $T \in [0, 10]$ and $s \in [-2, 10]$ is shown in Fig. 3 for the peptide in the vicinity of a substrate that is equally attractive for both hydrophobic and polar monomers. Solid lines visualize “paths” through the free energy landscape when changing temperature under constant solvent ($s = \text{const}$) conditions. Let us follow the exemplified trajectory for $s = 2.5$. Starting at very low temperatures, we know from the pseudo-phase diagram in Fig. 2(a) that the system resides in pseudo-phase AC1. This means that the macro-state of the peptide is dominated by the class of compact, film-like single-layer conformations. The system obviously prefers surface contacts at the expense of hydrophobic contacts. Nonetheless, the formation of compact hydrophobic domains in the two-dimensional topology is energetically favored but maximal compactness is hindered by the steric influence of the substrate-binding polar residues. Increasing the temperature, the system experiences close to $T \approx 0.35$ a sharp first-order-like conformational transition, and a second layer forms (AC2). This is a mainly entropy-driven transition as the extension into the third dimension perpendicular to the substrate surface increases the number of possible peptide conformations. Furthermore, the loss of energetically favored substrate contacts of polar monomers is partly compensated by the energetic gain due to the more compact hydrophobic domains. Increasing the temperature further, the density of the hydrophobic domains reduces and overall compact conformations dominate in the globular pseudo-phase AG. Reaching AE, the number of hydrophobic contacts decreases further, and also the total number of substrate contacts. Extended, dissolved conformations dominate. The transitions from AC2 to AE via AG are comparatively “smooth”, i.e., no immediate changes in the contact numbers passing the transition lines are noticed. Therefore, these conformational transitions could be classified as second-order-like. The situation is different when approaching the unbinding transition line from AE close to $T \approx 2.14$. This transition is accompanied by a dramatic loss of substrate contacts – the peptide desorbs from the substrate and behaves in pseudo-phase DE like a free peptide, i.e., only the substrate and the opposite neutral wall regularize the translational degree of freedom perpendicular to the walls, but rotational symmetries are unbroken (at least for conformations not touching one of the walls). As the probability distribution in Fig. 3 shows, the unbinding transition is also first-order-like, i.e., close to the transition line, there is a coexistence of adsorbing and desorbing classes of conformations.

6 Concluding Remarks

Summarizing, we have performed a detailed analysis of the pseudo-phase diagrams in the T - s plane for a selected heteropolymer with 103 monomers in cavities with an adsorbing substrate being either attractive independently of the monomer type, or selective to hydrophobic or polar monomers, respectively. Although our model is very simple and the focus is on hydrophobic and polar effects only, we find, beyond the expected adsorbed and desorbed phases, a rich subphase structure in the adsorbed phases. In these regions, the substrate-specificity depends in detail on the quality of the solvent.

Since current experimental equipment is capable to reveal molecular structures at the nanometer scale, it should be possible to investigate the grafted structures dependent on the solvent quality. This is essential for answering the question under what circumstances binding forces are strong enough to refold peptides or proteins. The vision of future biotechnological and medical applications is fascinating as it ranges from protein-specific sensory

devices to molecular electronic devices at the nanoscale.

Acknowledgments

This work is partially supported by a DFG (German Science Foundation) grant under contract No. JA 483/24-1. We thank the John von Neumann Institute for Computing (NIC), Forschungszentrum Jülich, for providing access to their supercomputer JUMP under grant No. hlz11.

References

1. S. Brown, *Nature Biotechnol.* **15**, 269 (1997).
2. S. R. Whaley, D. S. English, E. L. Hu, P. F. Barbara, A. M. Belcher, *Nature* **405**, 665 (2000); B. R. Pelle, E. M. Krauland, K. D. Wittrup, and A. M. Belcher, *Langmuir* **21**, 6929 (2005).
3. K. Goede, P. Busch, and M. Grundmann, *Nano Lett.* **4**, 2115 (2004).
4. R. L. Willett, K. W. Baldwin, K. W. West, and L. N. Pfeiffer, *Proc. Natl. Acad. Sci. (USA)* **102**, 7817 (2005).
5. T. Vrbová and S. G. Whittington, *J. Phys. A* **29**, 6253 (1996); *J. Phys. A* **31**, 3989 (1998); T. Vrbová and K. Procházka, *J. Phys. A* **32**, 5469 (1999).
6. Y. Singh, D. Giri, and S. Kumar, *J. Phys. A* **34**, L67 (2001); R. Rajesh, D. Dhar, D. Giri, S. Kumar, and Y. Singh, *Phys. Rev. E* **65**, 056124 (2002).
7. M. S. Causo, *J. Chem. Phys.* **117**, 6789 (2002).
8. J. Krawczyk, T. Prellberg, A. L. Owczarek, and A. Reznitzer, *Europhys. Lett.* **70**, 726 (2005).
9. J.-H. Huang and S.-J. Han, *J. Zhejiang Univ. SCI.* **5**, 699 (2004).
10. M. Bachmann and W. Janke, *Phys. Rev. Lett.* **95**, 058102 (2005).
11. K. F. Lau and K. A. Dill, *Macromolecules* **22**, 3986 (1989).
12. E. E. Lattman, K. M. Fiebig, and K. A. Dill, *Biochemistry* **33**, 6158 (1994).
13. L. Toma and S. Toma, *Prot. Sci.* **5**, 147 (1996).
14. H.-P. Hsu, V. Mehra, W. Nadler, and P. Grassberger, *J. Chem. Phys.* **118**, 444 (2003); *Phys. Rev. E* **68**, 21113 (2003).
15. M. Bachmann and W. Janke, *Phys. Rev. Lett.* **91**, 208105 (2003).
16. M. Bachmann and W. Janke, *Comp. Phys. Comm.* **169**, 111 (2005).
17. R. Schiemann, M. Bachmann, and W. Janke, *J. Chem. Phys.* **122**, 114705 (2005); *Comp. Phys. Comm.* **166**, 8 (2005).
18. M. Bachmann and W. Janke, *J. Chem. Phys.* **120**, 6779 (2004).
19. P. Grassberger, *Phys. Rev. E* **56**, 3682 (1997).
20. M. N. Rosenbluth and A. W. Rosenbluth, *J. Chem. Phys.* **23**, 356 (1955).